



Published in final edited form as:

*Biochem Pharmacol.* 2009 January 1; 77(1): 76–85. doi:10.1016/j.bcp.2008.09.011.

## THE ROLE OF GSH EFFLUX IN STAUROSPORINE-INDUCED APOPTOSIS IN COLONIC EPITHELIAL CELLS

Magdalena L. Circu<sup>1</sup>, Sarah Stringer<sup>1</sup>, Carol Ann Rhoads<sup>1</sup>, Mary Pat Moyer<sup>2</sup>, and Tak Yee Aw<sup>1,\*</sup>

<sup>1</sup>Department of Molecular & Cellular Physiology, Louisiana State University Health Science Center, Shreveport, LA 71130

<sup>2</sup>INCELL Corporation, San Antonio, TX 78249

### Abstract

Staurosporine (STP) was shown to induce cell apoptosis through formation of reactive oxygen species, but a role for cellular redox has not been defined. In this study, we report that STP (2 $\mu$ M) caused apoptosis (24 $\pm$ 3% at 24h) of human colon adenocarcinoma epithelial cell line HT29 that was preceded by significant GSH and GSSG efflux (6h), but independent of changes in cellular GSH/GSSG redox status. The blockade of GSH efflux by  $\gamma$ -glutamyl glutamate ( $\gamma$ -GG) or ophthalmic acid was associated with apoptosis attenuation; however,  $\gamma$ -GG administration after peak GSH efflux (8h) did not confer cytoprotection. Moreover, lowering cellular GSH through inhibition of its synthesis prevented extracellular GSH accumulation and cell apoptosis, thus validating a link between cellular GSH export and the trigger of cell apoptosis. Inhibition of  $\gamma$ -glutamyl transferase (GGT1 EC 2.3.2.2)-catalyzed extracellular GSH degradation with acivicin significantly blocked GSH efflux, suggesting that GSH breakdown is a driving force for GSH export. Interestingly, acivicin treatment enhanced extracellular GSSG accumulation, consistent with GSH oxidation. STP-induced HT29 cell apoptosis was associated with caspase-3 activation independent of caspase-8 or caspase-9 activity; accordingly, inhibitors of the latter caspases were without effect on STP-induced apoptosis. STP similarly induced GSH efflux and apoptosis in a nonmalignant human NCM460 colonic cell line in association with caspase-3 activation. Collectively, our results demonstrate that STP induction of apoptosis in malignant and non-malignant colonic cells is temporally linked to the export of cellular GSH and the activation of caspase-3 without caspase-8 or -9 involvement.

### Keywords

staurosporine and cell apoptosis; GSH efflux and cell apoptosis;  $\gamma$ -glutamyl transferase and GSH efflux; caspase-8 and -9 independent caspase-3 activation; extracellular GSH hydrolysis and GSH efflux; GSH efflux and caspase-3 activation

---

\* - Corresponding author. Address correspondence to: Tak Yee Aw, PhD, Department of Molecular & Cellular Physiology, LSU Health Sciences Center-Shreveport, 1501 Kings Highway, Shreveport, LA 71130-3932, USA, Tel: +01 318-675-6032, Fax: +01 318-675-4217, Email: taw@lsuhsc.edu.

**Publisher's Disclaimer:** This is a PDF file of an unedited manuscript that has been accepted for publication. As a service to our customers we are providing this early version of the manuscript. The manuscript will undergo copyediting, typesetting, and review of the resulting proof before it is published in its final citable form. Please note that during the production process errors may be discovered which could affect the content, and all legal disclaimers that apply to the journal pertain.

## 1. Introduction

Apoptosis plays an important role in homeostatic colon cell turnover, and defects in apoptosis are considered to contribute to the development of gut pathology [1,2], including villous atrophy, epithelial hyperplasia, loss of normal absorptive function and increased risk of tumorigenesis, such as colon cancer [3]. Oxidative stress, which generally correlates with a loss of cellular redox balance, has been implicated in the initiation of digestive disorders [4]. Glutathione is a key regulator of redox balance within cells [5], and cellular redox balance is a dynamic process that is achieved by maintenance of the glutathione/glutathione disulfide (GSH/GSSG) status [6]. Our recent studies with intestinal [3,4,7-9] and other cell types [10, 11] have shown that a loss of cellular GSH/GSSG redox balance is an important contributor to apoptotic signaling. In colonic cell apoptosis mediated by oxidants such as lipid hydroperoxides [4] and menadione [9], the initiation of apoptosis involves mitochondrial signaling in which the release of cytochrome *c* is temporally linked to the activation of caspase-9 and the downstream executioner caspase, caspase-3.

Interestingly, a role for oxidative stress has also been reported as a common mechanism in cell apoptosis for the non-oxidant, staurosporine (STP). STP is a broad spectrum, non specific inhibitor of cellular protein kinases, and has been widely used in induction of apoptosis in diverse cellular models [12-16]. In these studies, ROS production, dissipation of mitochondrial membrane potential, and the release of pro-apoptotic cytochrome *c* from mitochondria into the cytosol and downstream activation of the caspase cascade [16,17] have been shown to be involved in cell apoptosis. Given the association between oxidative stress and loss of cellular redox balance, these findings suggest that the intracellular GSH redox environment may be critical in STP-induced apoptosis. In other studies, GSH loss through efflux has been shown to be involved in Fas antibody and STP-induced apoptosis in Jurkat cells [18-20] that is independent of ROS formation [19]. Hammond et al [18] further demonstrated that apoptosis was significantly delayed in Raji cells (a lymphocyte cell line deficient in phosphatidylserine externalization) which did not release GSH, suggesting a role for GSH export in apoptosis activation and/or progression. At present, it is unknown as to whether STP induced apoptosis in colonic cells is mediated by cellular GSH loss through GSH efflux or through GSH oxidation.

The current study was undertaken to investigate the involvement of cellular GSH/GSSG and GSH efflux in STP-induced colonic cell apoptosis. Since STP has been shown to elicit differential susceptibility in primary cells (e.g., hepatocytes) and cancer cells of different tissue types (e.g., Huh-7, Jurkat) [21], we examined STP induced apoptosis in malignant HT29 as well as non-transformed NCM460 human colonic cell lines. A second objective was to investigate the participation of a novel caspase-3 pathway in STP induced human colonic cell apoptosis given that STP-induced hepatic apoptosis is mediated by a caspase-3 pathway which is independent of mitochondrial cytochrome *c* release and caspase-9 or caspase-8 activation [21]. Our results show that GSH efflux as driven by  $\gamma$ -glutamyl transferase-catalyzed extracellular GSH hydrolysis, is a major contributor to apoptosis initiation in both malignant and non-malignant colon cells induced by STP and did not involve changes in cellular GSH/GSSG redox status. We further report that induction of GSH efflux is temporally associated with caspase-3 activation that is independent of caspase-8 and caspase-9.

## 2. Materials and methods

### 2.1. Materials

The following chemicals were obtained from Sigma Chemical Corporation (St. Louis, MO): 4'6-diamidino-2-phenylindole (DAPI), staurosporine (STP),  $\gamma$ -glutamyl glutamate ( $\gamma$ -GG), 2,4-dinitrofluorobenzene, iodoacetic acid, glutathione (GSH), glutathione disulfide (GSSG), buthionine sulfoximine (BSO), acivicin, Triton X-100, mercaptoethanol, leupeptin, aprotinin,

dithiothreitol, PMSF, paraformaldehyde. Inhibitors of caspase 9 (LEHD-CHO) and caspase-8 (IETD-CHO) were from Calbiochem (San Diego, CA, USA). Ophthalmic acid (OPA) was purchased from Bachem Inc. (Torrance, CA). Antibiotic/antimycotic, L-glutamine, trypsin and Dulbecco's Modified Eagle Medium were obtained from GIBCO Corporation (Grand Isle, NY, USA). Fetal bovine serum was acquired from Atlanta Biologicals (Norcross, GA, USA). Polyclonal antibodies against caspase-9, caspase-3 (CPP-32), and cleaved caspase-3 (Asp175) were purchased from Cell Signaling (Danvers, MA). The antibody against caspase-8 was acquired from BD Biosciences (San Jose, CA, USA). The secondary IgG antibodies and the ECL plus Western blotting detection system were from Amersham (Arlington Heights, IL, USA). Nitrocellulose membranes and BioRad protein dye assay kit were obtained from BIORAD Corporation (Hercules, CA). M3:10 media was procured from INCELL Corporation (San Antonio, TX, USA). Fluorescence mounting medium was purchased from Dako Corporation (Carpinteria, CA, USA). Twelve mm circle number 1 glass cover slips were acquired from Fisher Corporation (Pittsburgh, PA, USA). The fluorescence caspase-3 assay kit was obtained from PharMingen (San Jose, CA, USA).

## 2.2. Cell culture and incubation

HT29 is a human colon adenocarcinoma epithelial cell line that was derived from the adenocarcinoma of the colon of a female Caucasian [22]. HT29 cells were purchased from American Type Culture Collection (Rockville, MD), and were grown in Dulbecco's Modified Eagle Medium (DMEM) supplemented with penicillin (100 units/ml), streptomycin (100 units/ml), and 10% fetal bovine serum. NCM460 is an immortalized and nonmalignant human colonic epithelial cell line [23] that was generated by Dr. Mary Moyer, INCELL Corporation. The NCM460 cell line was derived from the transverse colon of a human donor and exhibits characteristics similar to primary cultures of cells isolated from the same region [24]. The non-transformed colonocytes tested positive for the epithelial marker cytokeratin, the intestinal epithelial marker villin, the human secretory component and the colon-specific glycoprotein 5E113 [23]. Moreover, NCM460 cells exhibit transcripts for NHE-1 and NHE-2, but not NHE-3 isoforms [24]. NCM460 cells were cultured in M3:10 media. Both cell lines were maintained in a humidified incubator at 37°C in 5% CO<sub>2</sub>-95% air. The culture media were changed every 2 days and cells were plated in their respective growth media at a specified density one day before experimentation. On the day of the experiment, the media were replaced with DMEM (no phenol red, no FBS) and the reagents, whenever present, were added to the following final concentration: staurosporine (STP), 1µM (for NCM460) or 2µM (for HT29); γ-glutamyl glutamate (γ-GG), 10mM; ophthalmic acid (γ-glutamyl-amino isobutyric-glycine, OPA), 10mM; buthionine sulfoximine (BSO), 2mM; acivicin, 0.25 mM. Inhibitors of caspases-9 and -8 were each prepared as 20mM stock solutions in DMSO, and were added to cell cultures at final concentrations of 10µM.

## 2.3. Detection of apoptosis by DAPI staining

Cell apoptosis was visualized and quantified by DAPI staining as we previously described [25]. Briefly, 1×10<sup>5</sup> HT29 or NCM460 cells were plated on 12mm circular cover slips in 24-well plates and incubated overnight at 37°C in 5% CO<sub>2</sub>. The next day, cells were exposed to STP (1 for NCM460 and 2µM for HT29) for various times. In some wells, NCM460 and HT29 cells were pre-treated for 30min with 10mM γ-GG or OPA before treatment with STP. In other wells, HT29 cells were pretreated for 30min with 10µM LEHD-CHO or IETD-CHO (inhibitors of caspases-9 and -8, respectively) or for 24h with 2mM BSO prior to STP exposure. At the end of the experiments, cells were washed with PBS and fixed with 4% paraformaldehyde for 15min, and with 70% ethanol at -20°C for 1h. Cells on cover slips were stained with 1µg/ml DAPI for 30min in the dark, washed twice with PBS and mounted using DAKO fluorescence mounting fluid onto microscope slides. Cells were viewed and counted using a fluorescence Olympus B450 microscope with the 20× objective. At least 6 fields of total and apoptotic cells

were counted on each slide, and typically between 100 and 300 cells were counted in each field. Activation of caspases-9 and -8 as well as caspase-3 as respective markers of apoptosis initiation and execution were determined by western blot analysis (see below).

#### 2.4. Western blot analyses of procaspases-9, -8, and -3 activation

**Preparation of whole cell lysates**—HT29 or NCM460 cells ( $2 \times 10^6$ ) were seeded on 100mm plates and grown overnight at 37°C. Fresh media were added and cells were exposed to the designated STP concentrations for each cell line for different periods of time from 0 to 8h. After washing with PBS, cells were scraped and lysed in 0.3ml lysis buffer containing 300mM NaCl, 50mM Tris-HCl, 0.5% Triton X-100, 10µg/ml leupeptin, 10µg/ml aprotinin, 1mM PMSF, and 1mM dithiothreitol (DTT) for 30min at 4°C, and homogenized. The homogenates were centrifuged at 10,000 rpm and cell supernatants were stored at -20°C until Western blot analyses were performed.

**Western blot analyses**—Typically, 50µg of total protein extract was resolved on 12% acrylamide gels (100V, 90min) and blotted onto nitrocellulose membranes. The membranes were individually probed with primary and secondary antibodies at the following concentrations: Procaspase-8 (1:250; 1:1000); procaspase-9 (1:1000; 1:2000); procaspase-3 (CPP32, 1:500; 1:1000) and cleaved caspase-3 (1:1000; 1:2000). Chemiluminescence was detected with an ECL Western blotting detection reagent according to manufacturer's recommendation. Each membrane was stripped (6.25mM Tris pH 6.7, 2% SDS, 100mM mercaptoethanol) and reprobed for β-actin to verify equal protein loading per lane.

#### 2.5. Fluorometric determination of caspase-3 activity

HT29 cells ( $2 \times 10^6$ ) were seeded in 60mm plates and grown overnight at 37°C. The next day, the media was changed to FBS- and phenol red-free DMEM and cells were exposed to 2µM STP for 2, 4, 6 and 8h. Cell lysates were prepared according to the caspase-3 assay kit protocol. Briefly, 0.5ml of lysis buffer (10mM Tris-HCl; 100mM NaH<sub>2</sub>PO<sub>4</sub>/NaHPO<sub>4</sub> [pH 7.5]; 130mM NaCl; 1% Triton X-100; 10mM NaPPi) were added to each sample, mixed and centrifuged at 14,000 rpm. The supernatants were saved for determination of caspase-3 activity. The assay mixtures contained 1ml HEPES, 50µl cell lysate and 10µl of the non-fluorescent caspase-3 substrate (DEVD-AMC [N-acetyl-Aspartate-Glutamate-Valine-Aspartate]-AMC [7-amino-4-methylcoumarin]), and incubations were carried out for 1h at 37°C. The fluorescent product AMC was determined using a BioRad VersaFluor™ fluorometer at excitation and emission wavelengths of 380nm and 470nm, respectively. Results are expressed as relative fluorescence unit (RFU) per 10<sup>6</sup>cells.

#### 2.6. Measurements of cellular and extracellular GSH and GSSG

NCM460 and HT29 colonic cells ( $2 \times 10^6$ ) were seeded overnight on 100mm dishes in their respective growth media. The next day, the media was removed and cells were treated with 4ml of serum-free DMEM containing the designated STP concentrations for each cell line. At various times, aliquots of extracellular DMEM media were collected and centrifuged at 1200rpm for 4 min. The particulate-free media were treated with ice-cold 5% trichloroacetic acid (TCA) final concentration, and the acid supernatants were frozen at -20°C for GSH quantification (see below). In parallel experiments, GSH/GSSG efflux was determined in the presence of γ-glutamyl glutamate and ophthalmic acid; cells were incubated with the inhibitors (10mM) for 30min prior to STP addition. In some experiments, HT29 cells were pretreated with 0.25mM acivicin for 30 min to inhibit γ-glutamyl transferase (γ-GT)-catalyzed extracellular GSH hydrolysis. In studies of combined acivicin and γ-GG treatment, cells were incubated sequentially with each agent for 30min prior to STP addition. In each instance, media were collected at the same designated time points as control incubations for processing and

determination of extracellular GSH and GSSG levels. At time points corresponding to media sampling (i.e., 0-10h), cells were washed with PBS and harvested by scraping into ice-cold 5% TCA. Cell suspensions were centrifuged to remove TCA-insoluble proteins, and the acid supernatants were collected for quantification of intracellular GSH and GSSG concentrations.

**High-performance liquid chromatography (HPLC)**—Total GSH and GSSG contents were quantified by HPLC as previously described [26]. Acid supernatants were derivatized with 6mM iodoacetic acid and 1% 2,4-dinitrophenyl fluorobenzene to yield S-carboxymethyl and 2,4-dinitrophenyl derivatives of GSH/GSSG, respectively which were separated on a 250mm × 4.6 mm Alltech Lichrosorb NH2 10micron column. GSH and GSSG contents were quantified by comparison to standards derivitized in the same manner.

## 2.7. Protein assay

Protein was measured using Bio-Rad Protein Assay kit (Bio-Rad Laboratories, Hercules, CA, USA) according to the manufacture's protocol.

## 2.8. Statistical analysis

Results are expressed as mean ± SE. Data were analyzed using a one-way ANOVA with Bonferroni corrections for multiple comparisons. p values of <0.05 were considered as statistically significant.

## 3. Results

### 3.1. Staurosporine induced apoptosis in HT29 cells and the relationship to cellular GSH efflux

Figure 1 summarizes the effect of STP on apoptosis of HT29 cells and the relationship to cellular and extracellular GSH and GSSG status. Figure 1A shows that STP caused a time dependent increase in HT29 apoptosis that was significant at 8h and 24h. The increase in cell apoptosis correlated with STP-induced time-dependent decreases in cellular GSH and GSSG levels from 4h to 10h (Figure 1B). The cellular GSH-to-GSSG ratio was minimally altered by STP exposure (data not shown) which suggests a lack of GSH oxidation and oxidative stress associated with STP exposure. Notably, the loss of cellular GSH and GSSG was accompanied by their quantitative increases in the extracellular media (Figure 1C), consistent with STP-induced GSH and GSSG efflux. Extracellular GSH was significantly elevated at 6h post STP exposure and reached peak values at 8-10h that corresponded to an efflux of ~20% of total cellular GSH, while extracellular GSSG accumulation was significant at 8 and 10h (Figure 1C).

### 3.2. Inhibitors of GSH transport and GSH synthesis attenuate GSH efflux and STP-induced HT29 apoptosis

Since HT29 apoptosis was preceded by the loss of cellular GSH and GSSG that were quantitatively recovered in the extracellular media, we hypothesized that the export of GSH and/or GSSG may be the trigger for STP-induced cell apoptosis. To test this, we manipulated GSH efflux in two ways. First, GSH transport was inhibited using  $\gamma$ -GG or OPA [27]. The results show that  $\gamma$ -GG or OPA significantly attenuated the appearance of extracellular GSH (Figure 2A) and accordingly, afforded marked protection of HT29 cells against STP induced apoptosis (Figure 2B). However,  $\gamma$ -GG addition at 8h post STP treatment at a time after the peak of GSH efflux (see Figure 1C), did not confer cytoprotection (Figure 2C), which was consistent with a role for GSH export. Notably, the loss of cellular GSSG and its appearance in the media were unaffected by  $\gamma$ -GG (see Figure 5B), suggesting that GSSG export played a minimal role in the apoptotic process. Second, cellular GSH synthesis was inhibited as a means to decrease cytosolic GSH and GSH export. BSO treatment for 24h resulted in 10-fold attenuation in intracellular GSH concentrations (Figure 3A) which directly corresponded to



similar decreases in extracellular GSH levels (Figure 3B). Interestingly, even at this low intracellular GSH, the addition of STP for 8h caused a further decrease that was reflected in the extracellular concentration of GSH (Figure 3A & B), indicating that GSH efflux and extracellular GSH accumulation are directly linked to the intracellular GSH status. Figure 3C shows that BSO treatment significantly protected against STP-induced HT29 apoptosis at 24h in accordance with the attenuation in GSH efflux (Figure 3B), thus validating an association of GSH efflux and STP-induced HT29 apoptosis.

### 3.3. Inhibition of $\gamma$ -glutamyl transferase-catalyzed extracellular GSH hydrolysis attenuate STP-induced GSH efflux

To gain a better insight into the control of GSH efflux, we inhibited  $\gamma$ -glutamyl transferase ( $\gamma$ -GT, GGT1 EC 2.3.2.2) activity to test whether inhibition of extracellular GSH degradation can influence its export from cells. The results show that acivicin treatment blocked STP-induced loss of cellular GSH and significantly attenuated the appearance of GSH in the extracellular media (Figure 4A), suggesting that  $\gamma$ -GT-catalyzed GSH hydrolysis was a driving force for cellular GSH efflux. In contrast, acivicin did not prevent STP-induced decrease in cellular GSSG (Figure 4B), but caused time-dependent increases in extracellular GSSG levels (Figure 4B). Moreover, the effect of acivicin in attenuating STP-induced extracellular GSH accumulation and preventing cellular GSH decrease was quantitatively similar to that elicited by direct inhibition of GSH transport with  $\gamma$ -GG (Figure 5A). Combined acivicin and  $\gamma$ -GG treatment did not prevent further decrease in cellular GSH or extracellular GSH accumulation (Figure 5A), indicating that maximal blockade of GSH export was achieved with acivicin or  $\gamma$ -GG alone. As it is with  $\gamma$ -GG, acivicin exerted minimal effect on cellular GSSG loss; however, in contrast to  $\gamma$ -GG, acivicin induced significant extracellular GSSG accumulation alone or in combination with  $\gamma$ -GG (Figure 5B).

### 3.4. Staurosporine induces caspase-3 activation in HT29 cells independent of caspases-8 and -9

Given the centrality of caspase-3 activation in the execution of apoptosis, we determined its activation and temporal relationship to STP-induced efflux of GSH. Caspase-3 activation was assessed by the cleavage of procaspase-3 (CPP32) as well as the increase in caspase-3 activity. The results in Figure 6A show that STP induced a decrease in CPP32 expression between 6-8h (upper panel), consistent with cleavage of the pro-enzyme. Direct assay of caspase-3 activity confirmed the increase in enzyme activity beginning at 4h and reached maximum between 6h and 8h (Figure 6A, middle panel). The correspondence of the kinetics of caspase-3 activation to the peak of GSH efflux (see Figure 1C) suggests a temporal link between GSH loss and apoptosis initiation. To test whether STP mediated apoptosis resulted from mitochondria- or death receptor-initiated signals amplified through the mitochondria, we treated cells with inhibitors of caspase-9 or -8, the respective inhibitors of the mitochondria or death receptor pathways [28]. Interestingly, western blot analyses show that neither procaspase-8 (55kDa) nor procaspase-9 (47kDa) was activated over the 8h treatment with STP (Figure 6A, lower panel). Moreover, STP-induced HT29 apoptosis was unaffected by either inhibitors of caspase-9 or -8 (Figure 6B). These results suggest that STP-induced caspase-3 activation occurs by a mechanism that is independent of caspases-8 and -9, in agreement with previous studies in hepatocytes [21].

### 3.5. Staurosporine induces NCM460 cell apoptosis in association with cellular GSH efflux and activation of caspase-3

To examine whether STP-mediated apoptosis in non-malignant colon cells through induction of GSH efflux, we determined the effect of STP on apoptosis and the temporal relationships to cellular and extracellular GSH levels in NCM460 cells, an immortalized, nonmalignant

human colonic epithelial cell line that exhibits characteristics of primary cells [24]. Figure 7A shows that 1  $\mu$ M STP induced significant NCM460 cell apoptosis at 24h ( $25 \pm 4\%$ ); at 2  $\mu$ M, STP caused  $> 80\%$  NCM460 apoptosis at 24h (data not shown). STP-induced apoptosis was preceded by time-dependent increases in extracellular GSH between 2h and 6h (Figure 7B) and parallel decreases in cellular GSH not associated with changes in GSH-to-GSSG ratios (data not shown). Pretreatment with  $\gamma$ -GG significantly attenuated STP-induced NCM460 apoptosis (Figure 7A) in association with the blockade of GSH efflux (Figure 7C), supporting a link between STP induction of GSH efflux and NCM460 cell apoptosis. Figure 7D shows that the expression of procaspase-3 was low in untreated NCM460 cells in agreement with other cell types [11]. STP caused an increase in CPP32 expression at 4h followed by significant decreases at 6-8h (Figure 7D, upper left panel), consistent with initial mitochondria-to-cytosolic release of procaspase-3 followed by cleavage of the pro-enzyme to its active form. The marked decreases in CPP32 expression at 6-8h directly correlated with significant increases in the appearance of cleaved caspase-3 at these times (19 and 17 kDa, Figure 7D, lower left panel). Neither procaspases -8 or -9 were activated over 8h STP exposure (Figure 7D, right panel).

#### 4. Discussion

The current study demonstrates that efflux of cellular GSH following STP exposure is an important contributor to apoptosis initiation in malignant HT29 and non-malignant NCM460 colonic epithelial cells which occurs independently of the cellular GSH-to-GSSG redox status. These conclusions are supported by several lines of evidence. First, the lack of a role for cellular oxidative stress is evidenced by lack of an increase in intracellular GSSG or a change in the GSH/GSSG ratio (Figure 1B, 5C), suggesting minimal ROS formation. The findings that (a) decreasing cellular GSH with BSO prevented extracellular GSH accumulation and (b) that blockade of GSH efflux with  $\gamma$ -GG or OPA prevented GSH efflux which was concomitant with attenuated apoptosis support the conclusion that STP-induced GSH efflux is critical in cell apoptosis. Furthermore, the failure of  $\gamma$ -GG to protect against cell apoptosis (at 24h) when added at a time after peak GSH efflux (at 8h) suggests that the export of GSH induced by STP is more likely associated with an activation event in apoptosis initiation rather than apoptosis progression. Our results suggest that GSH export is driven by its enzymatic degradation by  $\gamma$ -glutamyl transferase and are kinetically consistent with a coupling of GSH export to caspase-3 activation and apoptosis execution within the first 8h of STP exposure; subsequent blockade of GSH efflux was ineffective in preventing apoptosis progression to its biological endpoint at 24h.

Recent studies have implicated GSH export as a mechanism of STP-induced apoptosis in Jurkat cells [18]. Additionally, GSH loss and its extracellular accumulation was also associated with FasL/death receptor mediated progression of the execution phase of Jurkat cell apoptosis [20]. The extrusion of cellular GSH during FasL- or STP-induced apoptosis was mediated by the multidrug resistance-associated proteins, ABCC/MRP, and the organic anion-transport polypeptide protein (SLCO/OATP) which served as transport mechanisms for GSH loss [18, 19] that triggered phosphatidylserine externalization. Whether these GSH transport proteins function in STP induced GSH efflux and colonic cell apoptosis is unknown. Our current observation shows that GSH efflux induced by STP was not associated with oxidative stress and induction of GSH/GSSG redox imbalance, in agreement with previous findings that death receptor-mediated loss of GSH was similarly independent of ROS generation [19]. However, in other cell models [29-31], STP exposure was linked to ROS production and oxidative stress [32,33], phosphatidylserine externalization [34], DNA fragmentation [15], mitochondrial membrane depolarization and cytochrome *c* release into the cytosol [16,17]. Thus, the generality for a role for oxidative stress in STP-induced apoptosis remains unresolved and its importance may be cell type specific or a function of STP dose.

While there was a lack of involvement of the cellular GSH/GSSG redox state in STP-induced cell apoptosis, the cellular GSH pool size was important in determining extracellular GSH accumulation in STP-induced cell apoptosis, as evidenced by the finding that lowering cellular GSH with BSO prevented extracellular GSH accumulation. That inhibition of GSH synthesis and extracellular export with BSO significantly protected colonic cells against STP affirms our suggestion that intracellular GSH determines extracellular GSH export which is central in the mechanism of STP-induced cell apoptosis. Our result that acivicin, an irreversible inhibitor of  $\gamma$ -GT activity [35] preserved cellular GSH and attenuated GSH efflux is consistent with the notion that  $\gamma$ -GT-mediated extracellular GSH hydrolysis is an important driving force for GSH extrusion. This interpretation is supported by the results that sequential exposure of intestinal cells to acivicin followed by  $\gamma$ -GG did not result in additional extracellular GSH decrease suggesting that maximal efflux was  $\gamma$ -GT-driven. Interestingly, acivicin exerted no effect on cellular GSSG loss which indicates that GSSG efflux per se is independent of  $\gamma$ -GT. However,  $\gamma$ -GT inhibition significantly induced time-dependent increases in extracellular GSSG (Figure 4B,5B), possibly due to enhanced oxidation of extracellular GSH in the absence of GSH hydrolysis by plasma membrane-associated quiescin-sulphydryl oxidases [36].

The observation that activation of caspase-3 by STP-induced GSH efflux was not associated with caspases-8 or -9 activation, indicates a distinct caspase-3 pathway from the classical mitochondrial and receptor mediated, mitochondrial amplification mechanism of apoptosis execution. This result in colonic cells agrees with previous description of a novel caspase-3 pathway in STP-induced hepatocyte apoptosis that was not dependent on the function of caspase-8 or caspase-9 [21]. Taken together, these results suggest that activation of caspase-3 by a unique pathway not involving classical caspases-8 or -9 may be a general mechanism of STP-induced apoptosis in the liver and colon. The question of how GSH efflux initiates apoptotic signaling that is tied to activation of caspase-3 is unclear and warrants further investigation. One possibility may be related to GSH stimulation of receptor mediated signaling through accumulated extracellular GSH that alters the extracellular thiol/disulfide status. Our previous studies [37] and others [38] have demonstrated that colonic cell proliferation is, indeed influenced by the extracellular redox potential. A second possibility may be a direct modulation of cell surface membrane receptors or proteins by S-glutathionylation from accumulated extracellular GSH, a suggestion that awaits future validation.

Another notable observation is the greater sensitivity of NCM460 cells than HT29 cells to STP challenge, given that 1 $\mu$ M STP elicited the same degree of apoptosis in NCM460 cells as 2 $\mu$ M STP did in HT29 cells, consistent with the notion that STP induces differential susceptibility in cancer and non-cancer colon cells. This greater sensitivity and responsiveness of NCM460 cells to STP corresponded to kinetically faster and quantitatively higher GSH export at earlier times (2-6h) after STP exposure that correlated with similar early kinetics of caspase-3 activation (6h). Thus, it appears that STP-induced vulnerability of non-transformed colon cells is a function of the magnitude and faster kinetics of cellular GSH loss through efflux. However, despite greater sensitivity of NCM460 cells to STP, the qualitative similarity of GSH efflux as mechanism in STP-induced activation of a non-classical caspase-3 pathway suggests that STP mediates similar signaling events in cancer and non cancer colon cells. Interestingly, decreased sensitivity to STP has been reported for non-transformed and non-proliferating primary cultures of murine hepatocytes as compared to malignant Huh-7 and Jurkat cells [21]. Whether extracellular/intracellular GSH play a role in this differential susceptibility was not determined. In summary, we have demonstrated that GSH efflux independent of cellular GSH/GSSG redox change, is an important contributor to STP-induced colonic cell apoptosis wherein non-transformed colon cells are more vulnerable in accordance with a greater magnitude and faster kinetics of GSH efflux. Our results further point to  $\gamma$ -glutamyl transferase-catalyzed GSH hydrolysis as a major driving force for GSH export and to a non-classical pathway for caspase-3 activation in STP-induced apoptosis execution that



was independent of caspase-8 and caspase-9 function. At present, the biological significance of sensitization of non-transformed colon cells to STP and the involvement of a distinct caspase-3 pathway in STP induced colon cell death is unclear.

## Acknowledgements

We wish to thank Cynthia McNutt Rodriguez for careful editing of the manuscript. This study was supported by a grant from the National Institutes of Health, DK 44510.

## References

1. Que FG, Gores GJ. Cell death by apoptosis: basic concepts and disease relevance for the gastroenterologist. *Gastroenterology* 1996;110:1238–43. [PubMed: 8613014]
2. Watson AJ. Review article: manipulation of cell death--the development of novel strategies for the treatment of gastrointestinal disease. *Aliment Pharmacol Ther* 1995;9:215–26. [PubMed: 7654884]
3. Iwakiri R, Gotoh Y, Noda T, Sugihara H, Fujimoto K, Fuseler J, et al. Programmed cell death in rat intestine: effect of feeding and fasting. *Scand J Gastroenterol* 2001;36:39–47. [PubMed: 11218238]
4. Wang TG, Gotoh Y, Jennings MH, Rhoads CA, Aw TY. Lipid hydroperoxide-induced apoptosis in human colonic CaCo-2 cells is associated with an early loss of cellular redox balance. *Faseb J* 2000;14:1567–76. [PubMed: 10928991]
5. Aw TY. Molecular and cellular responses to oxidative stress and changes in oxidation-reduction imbalance in the intestine. *Am J Clin Nutr* 1999;70:557–65. [PubMed: 10500026]
6. Murphy ME, Scholich H, Sies H. Protection by glutathione and other thiol compounds against the loss of protein thiols and tocopherol homologs during microsomal lipid peroxidation. *Eur J Biochem* 1992;210:139–46. [PubMed: 1446667]
7. Noda T, Iwakiri R, Fujimoto K, Aw TY. Induction of mild intracellular redox imbalance inhibits proliferation of CaCo-2 cells. *Faseb J* 2001;15:2131–9. [PubMed: 11641239]
8. Noda T, Iwakiri R, Fujimoto K, Yoshida T, Utsumi H, Sakata H, et al. Suppression of apoptosis is responsible for increased thickness of intestinal mucosa in streptozotocin-induced diabetic rats. *Metabolism* 2001;50:259–64. [PubMed: 11230775]
9. Circu ML, Rodriguez C, Maloney R, Moyer MP, Aw TY. Contribution of mitochondrial GSH transport to matrix GSH status and colonic epithelial cell apoptosis. *Free Radic Biol Med* 2008;44:768–78. [PubMed: 18267208]
10. Okouchi M, Okayama N, Aw TY. Differential susceptibility of naive and differentiated PC-12 cells to methylglyoxal-induced apoptosis: influence of cellular redox. *Curr Neurovasc Res* 2005;2:13–22. [PubMed: 16181096]
11. Ekshyyan O, Aw TY. Decreased susceptibility of differentiated PC12 cells to oxidative challenge: relationship to cellular redox and expression of apoptotic protease activator factor-1. *Cell Death Differ* 2005;12:1066–77. [PubMed: 15877105]
12. Tamaoki T, Nomoto H, Takahashi I, Kato Y, Morimoto M, Tomita F. Staurosporine, a potent inhibitor of phospholipid/Ca<sup>++</sup>dependent protein kinase. *Biochem Biophys Res Commun* 1986;135:397–402. [PubMed: 3457562]
13. Ruegg UT, Burgess GM. Staurosporine, K-252 and UCN-01: potent but nonspecific inhibitors of protein kinases. *Trends Pharmacol Sci* 1989;10:218–20. [PubMed: 2672462]
14. Belmokhtar CA, Torriglia A, Counis MF, Courtois Y, Jacquemin-Sablon A, Segal-Bendirdjian E. Nuclear translocation of a leukocyte elastase Inhibitor/Elastase complex during staurosporine-induced apoptosis: role in the generation of nuclear L-DNase II activity. *Exp Cell Res* 2000;254:99–109. [PubMed: 10623470]
15. Yuste VJ, Sanchez-Lopez I, Sole C, Moubarak RS, Bayascas JR, Dolcet X, et al. The contribution of apoptosis-inducing factor, caspase-activated DNase, and inhibitor of caspase-activated DNase to the nuclear phenotype and DNA degradation during apoptosis. *J Biol Chem* 2005;280:35670–83. [PubMed: 16049016]

16. Smali SS, Hsu YT, Sanders KM, Russell JT, Youle RJ. Bax translocation to mitochondria subsequent to a rapid loss of mitochondrial membrane potential. *Cell Death Differ* 2001;8:909–20. [PubMed: 11526446]
17. Tafani M, Cohn JA, Karpinich NO, Rothman RJ, Russo MA, Farber JL. Regulation of intracellular pH mediates Bax activation in HeLa cells treated with staurosporine or tumor necrosis factor-alpha. *J Biol Chem* 2002;277:49569–76. [PubMed: 12393866]
18. Hammond CL, Marchan R, Krance SM, Ballatori N. Glutathione export during apoptosis requires functional multidrug resistance-associated proteins. *J Biol Chem* 2007;282:14337–47. [PubMed: 17374608]
19. Franco R, Panayiotidis MI, Cidlowski JA. Glutathione depletion is necessary for apoptosis in lymphoid cells independent of reactive oxygen species formation. *J Biol Chem* 2007;282:30452–65. [PubMed: 17724027]
20. Franco R, Cidlowski JA. SLCO/OATP-like transport of glutathione in FasL-induced apoptosis: glutathione efflux is coupled to an organic anion exchange and is necessary for the progression of the execution phase of apoptosis. *J Biol Chem* 2006;281:29542–57. [PubMed: 16857677]
21. Feng G, Kaplowitz N. Mechanism of staurosporine-induced apoptosis in murine hepatocytes. *Am J Physiol Gastrointest Liver Physiol* 2002;282:G825–34. [PubMed: 11960779]
22. von Kleist S, Chany E, Burtin P, King M, Fogh J. Immunohistology of the antigenic pattern of a continuous cell line from a human colon tumor. *J Natl Cancer Inst* 1975;55:555–60. [PubMed: 1159834]
23. Moyer MP, Manzano LA, Merriman RL, Stauffer JS, Tanzer LR. NCM460, a normal human colon mucosal epithelial cell line. *In Vitro Cell Dev Biol Anim* 1996;32:315–7. [PubMed: 8842743]
24. Sahi J, Nataraja SG, Layden TJ, Goldstein JL, Moyer MP, Rao MC. Cl- transport in an immortalized human epithelial cell line (NCM460) derived from the normal transverse colon. *Am J Physiol* 1998;275:C1048–57. [PubMed: 9755058]
25. Wang X, Martindale JL, Liu Y, Holbrook NJ. The cellular response to oxidative stress: influences of mitogen-activated protein kinase signalling pathways on cell survival. *Biochem J* 1998;333(Pt 2): 291–300. [PubMed: 9657968]
26. Reed DJ, Babson JR, Beatty PW, Brodie AE, Ellis WW, Potter DW. High-performance liquid chromatography analysis of nanomole levels of glutathione, glutathione disulfide, and related thiols and disulfides. *Anal Biochem* 1980;106:55–62. [PubMed: 7416469]
27. Ballatori N, Dutcak WJ. Identification and characterization of high and low affinity transport systems for reduced glutathione in liver cell canalicular membranes. *J Biol Chem* 1994;269:19731–7. [PubMed: 8051053]
28. Pias, EK.; Aw, TY. Mechanisms of parenchymal apoptosis. Schmid-Schonbein, GW.; Granger, DN., editors. Springer; Verlag: 2003. p. 297-309.
29. Andersson M, Sjostrand J, Petersen A, Honarvar AK, Karlsson JO. Caspase and proteasome activity during staurosporin-induced apoptosis in lens epithelial cells. *Invest Ophthalmol Vis Sci* 2000;41:2623–32. [PubMed: 10937575]
30. Sunaga S, Kobayashi T, Yoshimori A, Shiokawa D, Tanuma S. A novel inhibitor that protects apoptotic DNA fragmentation catalyzed by DNase gamma. *Biochem Biophys Res Commun* 2004;325:1292–7. [PubMed: 15555567]
31. Campello S, De Marchi U, Szabo I, Tombola F, Martinou JC, Zoratti M. The properties of the mitochondrial megachannel in mitoplasts from human colon carcinoma cells are not influenced by Bax. *FEBS Lett* 2005;579:3695–700. [PubMed: 15963994]
32. Seleznev K, Zhao C, Zhang XH, Song K, Ma ZA. Calcium-independent phospholipase A2 localizes in and protects mitochondria during apoptotic induction by staurosporine. *J Biol Chem* 2006;281:22275–88. [PubMed: 16728389]
33. Gil J, Almeida S, Oliveira CR, Rego AC. Cytosolic and mitochondrial ROS in staurosporine-induced retinal cell apoptosis. *Free Radic Biol Med* 2003;35:1500–14. [PubMed: 14642398]
34. Matura T, Serinkan BF, Jiang J, Kagan VE. Phosphatidylserine peroxidation/externalization during staurosporine-induced apoptosis in HL-60 cells. *FEBS Lett* 2002;524:25–30. [PubMed: 12135736]
35. Stole E, Smith TK, Manning JM, Meister A. Interaction of gamma-glutamyl transpeptidase with acivicin. *J Biol Chem* 1994;269:21435–9. [PubMed: 7914892]

36. Heckler EJ, Rancy PC, Kodali VK, Thorpe C. Generating disulfides with the Quiescin-sulfhydryl oxidases. *Biochim Biophys Acta* 2008;1783:567–77. [PubMed: 17980160]
37. Noda T, Iwakiri R, Fujimoto K, Rhoads CA, Aw TY. Exogenous cysteine and cystine promote cell proliferation in CaCo-2 cells. *Cell Prolif* 2002;35:117–29. [PubMed: 11952646]
38. Miller LT, Watson WH, Kirlin WG, Ziegler TR, Jones DP. Oxidation of the glutathione/glutathione disulfide redox state is induced by cysteine deficiency in human colon carcinoma HT29 cells. *J Nutr* 2002;132:2303–6. [PubMed: 12163679]

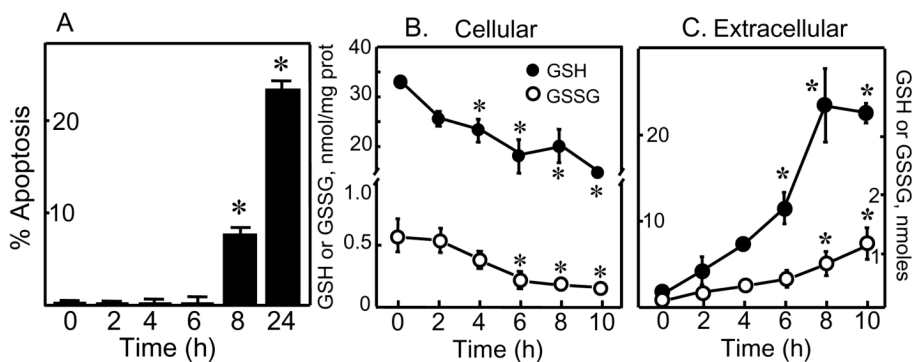


**Figure 1. STP induces HT29 cells apoptosis through cellular GSH efflux**

**A:** HT29 cells were exposed to 2 $\mu$ M STP for various times and apoptosis was determined by DAPI staining as described in Materials and Methods. Results are expressed as mean  $\pm$  S.E. GSH and GSSG contents in cells and extracellular media were determined at 0-10h after 2 $\mu$ M STP treatment. **B:** Intracellular GSH or GSSG expressed as nmoles/mg protein are presented as mean  $\pm$  S.E. for 4 separate experiments. **C:** GSH or GSSG in extracellular media are expressed as total contents in nmoles and presented as mean  $\pm$  S.E. for 4 separate experiments. \*p< 0.05 versus 0h control.

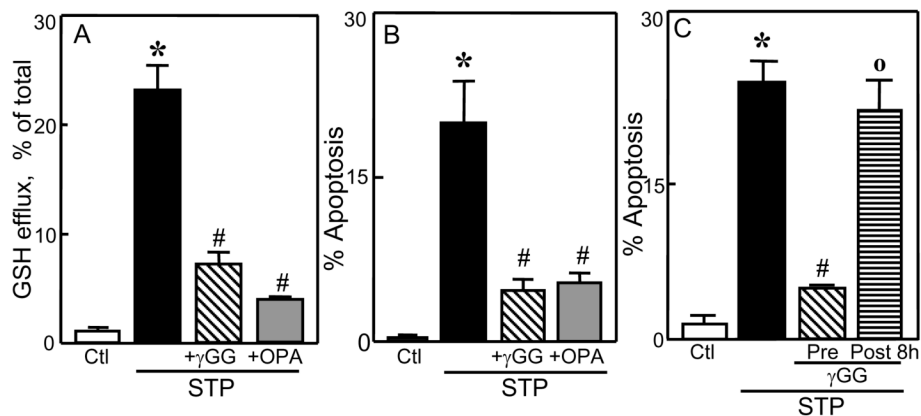


**Figure 2. Inhibitors of cellular GSH efflux attenuates STP-induced apoptosis**

HT29 cells were treated for 8h with  $2\mu\text{M}$  STP without or with 30min pre-treatment with 10mM of each of the GSH transport inhibitors,  $\gamma$ -glutamyl glutamate ( $\gamma\text{GG}$ ) or ophthalmic acid (OPA). Total GSH in the extracellular media and cell apoptosis were determined at 8h and 24h, respectively, post STP treatment. **A:** Percent GSH efflux. **B:** Percent cell apoptosis. Results are mean  $\pm$  S.E. for 4 separate experiments \*  $p < 0.05$  versus untreated control; #  $p < 0.05$  versus STP alone. **C:** HT29 cells were treated with  $2\mu\text{M}$  STP and cell apoptosis was determined at 24h. In some experiments,  $\gamma\text{GG}$  (10mM) were added either at 30min before or at 8h post-STP treatment. Results are mean  $\pm$  S.E. \*  $p < 0.05$  versus untreated control; #  $p < 0.05$  versus STP alone, °  $p < 0.05$  versus 30min pretreatment with  $\gamma$ -GG before STP exposure.



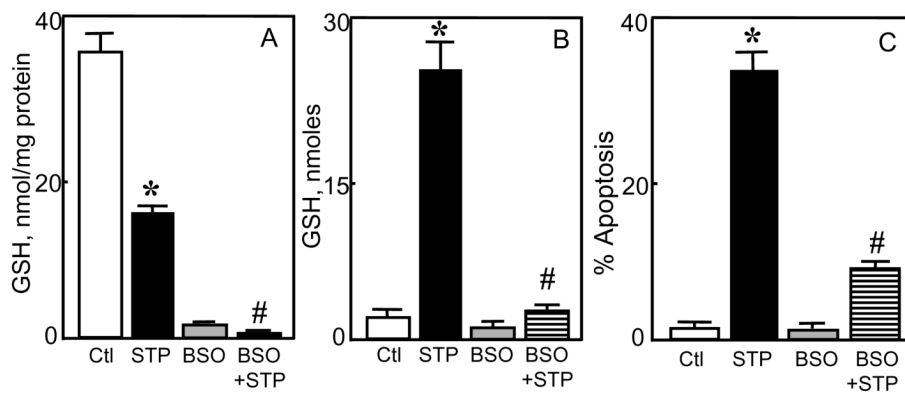


**Figure 3. Inhibitor of cellular GSH synthesis attenuates STP-induced GSH efflux and HT29 cell apoptosis**

HT29 cells were treated with 2 μM STP without or with 24h pre-treatment with 2mM BSO. Cellular GSH and total GSH in the extracellular media were determined at 8h, and cell apoptosis at 24h post STP treatment. **A:** Cellular GSH, expressed as nmol/mg protein. **B:** Total GSH in the extracellular media, expressed as nmoles. **C:** Percent HT29 cell apoptosis. Data are expressed as mean ± S.E. for 4 separate experiments. \* p < 0.05 versus untreated control; # p < 0.05 versus STP alone. 24h pretreatment of cells with BSO alone decreased cellular GSH by 10-fold (panel A).

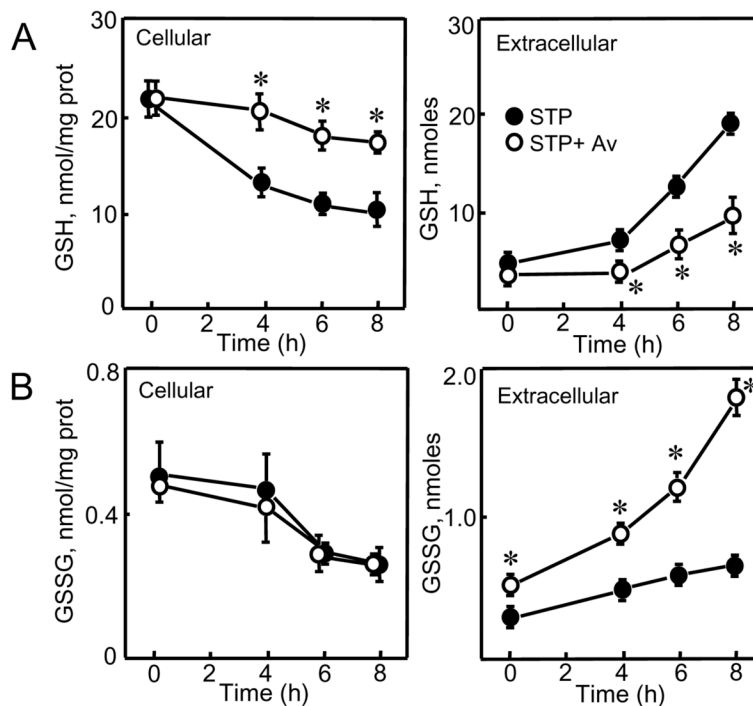


**Figure 4. Effect of acivicin on time course of loss of cellular GSH and GSSG and their accumulation in extracellular media**

HT29 cells were pretreated for 30min with 0.25mM acivicin (Av) followed by exposure to 2 $\mu$ M STP. Cellular and extracellular contents of GSH and GSSG were determined at specified times between 0-8h, and are expressed as nmoles/mg protein and nmoles, respectively. Results are mean  $\pm$  S.E. for 3 separate experiments. \* p < 0.05 versus corresponding times with STP alone.

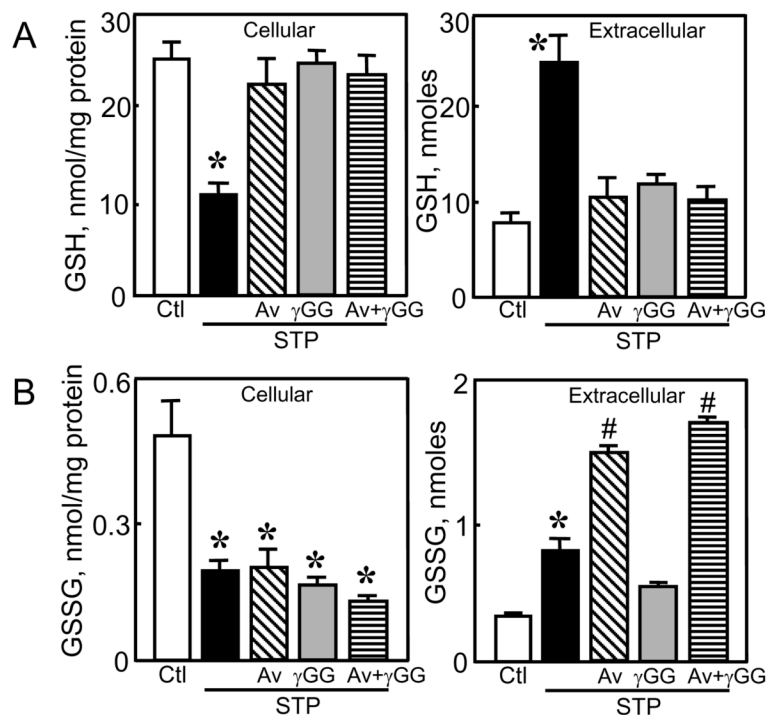


**Figure 5. Effect of acivicin and  $\gamma$ -glutamyl glutamate on loss of cellular GSH and GSSG and their accumulation in extracellular media**

HT29 cells were pretreated with either acivicin (Av, 0.25 mM),  $\gamma$ -glutamyl glutamate ( $\gamma$ GG, 10 mM), or combined Av and  $\gamma$ GG before STP addition as described in Materials and Methods. Cellular and extracellular contents of GSH and GSSG were determined at 8h, and are expressed as nmoles/mg protein and nmoles, respectively. Results are mean  $\pm$  S.E. for 3 separate experiments. \*  $p < 0.05$  versus untreated control; #  $p < 0.05$  versus STP alone.

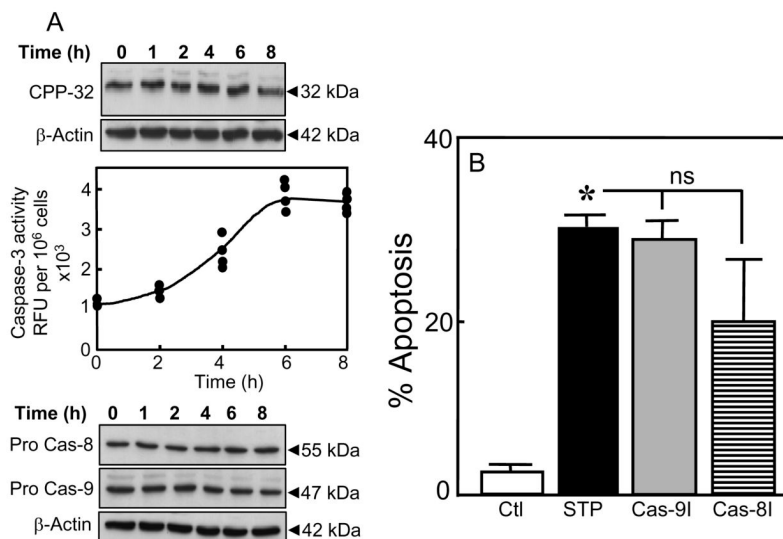


**Figure 6. STP induces caspase-3 activation that is independent of caspase-8 or caspase-9**  
 HT29 cells were incubated with 2 $\mu$ M STP for 0-8h, and total protein extracts were prepared. **A: Top panel**, western blot analysis of procaspase-3 (CPP32) expression; **Middle panel**, caspase-3 activity as determined by a fluorometric assay (see Materials and Methods). The results at each time point represent all data from two different assays performed in duplicates; **Bottom panel**, western blot analyses of caspases-8 and -9 expression. The membranes of each immunoblot were stripped and reprobed for  $\beta$ -actin to verify equal protein loading in each lane. One representative of 3 western blots is shown for each procaspase. **B:** HT29 cells were incubated with 2 $\mu$ M STP without or with 30min pretreatment with 10 $\mu$ M of pan caspase inhibitors of caspases-8 (Cas-8I, IETD-CHO) and -9 (Cas-9I, LEHD-CHO). Apoptosis was determined at 24h by DAPI staining. Results are mean  $\pm$  S.E. for 4 separate experiments \*  $p < 0.05$  versus untreated control.

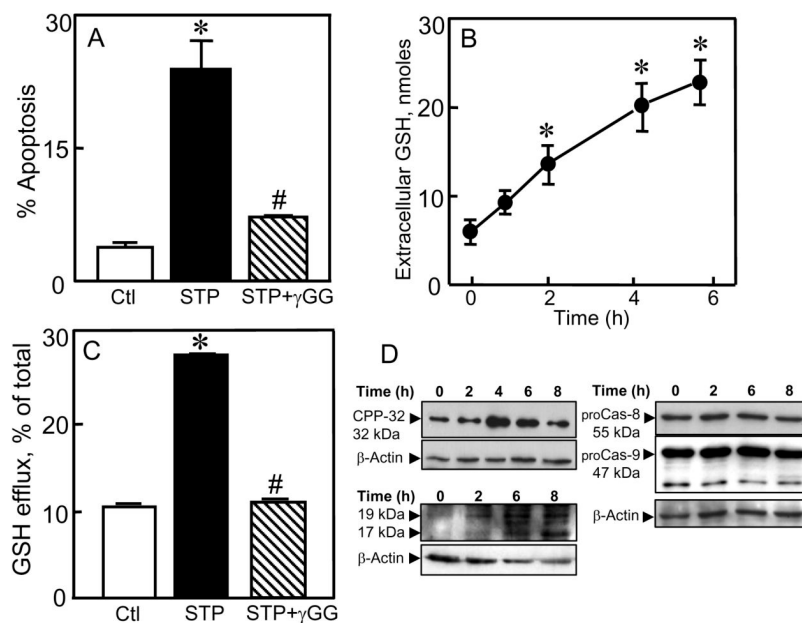


**Figure 7. STP-induced NCM460 cell apoptosis: Association with GSH efflux and caspase-3 activation**

NCM460 cells were exposed to 1  $\mu$ M STP without or with pretreatment (30min) with 10mM  $\gamma$ -glutamyl glutamate ( $\gamma$ GG). Apoptosis at 24h (A) and extracellular GSH contents at 6h (C) were determined. In other experiments, NCM460 cells were treated with 1  $\mu$ M STP, and at designated times between 0-6h, aliquots of extracellular media were sampled for determination of kinetics of GSH efflux (B). Cellular GSH and total extracellular GSH are expressed as expressed as nmol/mg protein and nmoles, respectively. Results are mean  $\pm$  S.E for 4 separate experiments. \* $p$ < 0.05 versus untreated control; # $p$ < 0.05 versus STP alone. **D:** NCM460 cells were incubated with 1  $\mu$ M STP for 0-8h, and total protein extracts were prepared for western blot analyses. **Left panels**, expression of procaspase-3 (CPP-32, Top) and cleaved caspase-3 (19 and 17 kDa bands, Bottom). **Right panel**, expression of procaspase-8 and procaspase-9. The membranes of each immunoblot were stripped and reprobbed for  $\beta$ -actin to verify equal protein loading in each lane. One representative of 3 western blots is shown for each procaspase.